ELSEVIER

Journal of Photochemistry and Photobiology A: Chemistry 110 (1997) 123–129

Journal of PHOTOCHEMISTRY AND PHOTOBIOLOGY A: CHEMISTRY

# Photophysical characterization of fluorenone derivatives

R.S. Murphy, C.P. Moorlag, W.H. Green, C. Bohne *

*Department of Chemistry, University of Victoria, P.O. Box 3065, Victoria, B.C., V8W 3V6, Canada*

Received 3 February 1997; revised 20 May 1997; accepted 2 June 1997

**Abstract**

The photophysics of several fluorenone derivatives was studied using fluorescence and laser-induced optoacoustic spectroscopy. Electron-donating substituents increase the energy of the key upper triplet state ($T_3$) which, for the parent compound, is responsible for the increased intersystem crossing quantum yield in non-polar solvents. Electron-withdrawing substituents decrease the energy of $T_3$, and an increase in the intersystem crossing rate constant is observed. Halogen substitution leads to a heavy-atom effect, which is partially compensated by a decrease in the intersystem crossing rate constant due to changes in the energy gap between $S_1$ and $T_3$. For most compounds, an increase in the internal conversion rate constant is observed. The magnitude of this increase is a function of the nature of the substituent and its position on the fluorenone ring. © 1997 Elsevier Science S.A.

*Keywords:* Fluorenone derivatives; Photophysics

## 1. Introduction

The photochemical reactivity of aromatic ketones is determined by the configuration of the lowest excited state. In hydrogen abstraction reactions, excited triplet ketones with $n,\pi^*$ configurations are much more reactive than triplet states with $\pi,\pi^*$ configurations [1]. Some aromatic ketones have excited states with different configurations, which are very close in energy. As a result, the configuration of the lowest excited state can be changed by the addition of electron-withdrawing or electron-donating substituents or by the use of solvents with different polarities.

Molecules having excited states with different configurations which are close in energy frequently exhibit complex reactivity and/or photophysical behavior. This complexity for fluorenone (Scheme 1) has long been established [2–5]. The influence of the solvent polarity on the configuration and energy of the lowest singlet excited state ($S_1$) and on its position relative to the upper triplet state (probably $T_3$) has been established by steady state and time-resolved picosecond fluorescence studies [6,7], laser flash photolysis experiments [8] and the investigation of the effect of the temperature on fluorenone photophysics [9]. In non-polar solvents, in which the $S_1$ state has an $n,\pi^*$ configuration, the fluorescence quantum yield is low, the fluorescence lifetime is short, the intersystem crossing quantum yield and rate constant are high and a temperature dependence is observed for the latter rate constant. In polar solvents, in which the $S_1$ state has a $\pi,\pi^*$ configuration, the fluorescence quantum yields and lifetimes increase. The intersystem crossing quantum yields are much smaller than those in non-polar solvents, and no temperature dependence is observed. In addition, internal conversion is a significant deactivation pathway for the singlet excited state. This behavior is primarily due to significant changes in the intersystem crossing rate constants in solvents of different polarity. In non-polar solvents, it is believed that $T_3$, which has an $n,\pi^*$ configuration and an energy comparable with that of $S_1$, is involved in the intersystem crossing process. In contrast, in polar solvents, the energy of $T_3$ is too high for this electronic state to participate in the crossing to the triplet surface. Furthermore, solvents capable of hydrogen bonding increase the internal conversion in fluorenone at the expense of fluorescence and triplet formation [10,11]. The photophysics of fluorenone can also be

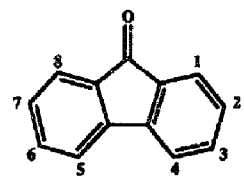


Scheme 1.

* Corresponding author. Tel.: +1 250 721 7151; fax: +1 250 721 7147; e-mail: Bohne@uvphys.phys.uvic.ca


*PII* S1010-6030(97)00191-3

affected when intramolecular hydrogen bonding is possible, as reported for 1-aminofluorenone [12,13].

In contrast with the reports on the photochemistry and photophysics of fluorenone, only limited data are available on the photophysics of substituted derivatives. The photophysics of 2-fluorofluorenone (**2FF**) parallels that of fluorenone. However, for 2-methoxyfluorenone, intersystem crossing is not affected by the polarity of the solvent. This is probably due to the higher dipole moment of the excited state when compared with the excited state dipole moment of fluorenone [14]. The importance of the charge transfer character of the excited states has also been implicated for nitro- and perester-fluorenones [15]. In this work, we report the photophysics of several fluorenone derivatives in order to gain further insight into how substituents affect the photophysics of this ketone.

## 2. Experimental details

### 2.1. Chemicals

9-Fluorenone (**FL**, Aldrich, 98%), 9-fluorenone-2-carboxylic acid (**F-2CA**, Aldrich, 98%), 9-fluorenone-4-carboxylic acid (**F-4CA**, Aldrich, 97%), 2-hydroxy-9-fluorenone (**2OHF**, Aldrich), 2,7-dibromo-9-fluorenone (**2,7DBF**, Aldrich, 96%), 2,7-dichloro-9-fluorenone (**2,7DCF**, Aldrich, 90%) and *ortho*-hydroxybenzophenone (Aldrich, 99%) were recrystallized from ethanol and water. 1,3-Dichloro-9-fluorenone (**1,3DCF**, ABC library, Aldrich), 2,7-difluoro-9-fluorenone (**2,7DFF**, ABC library, Aldrich), 3-hydroxy-9-fluorenone (**3OHF**, ABC library, Aldrich), 4-hydroxy-9-fluorenone (**4OHF**, Aldrich, 98%), 4-methoxy-9-fluorenone (**4MF**, ABC library, Aldrich), acetonitrile (ACP chemicals, spectrograde) and toluene (ACP chemicals, spectrograde) were used as received.

### 2.2. Absorption

Ground state UV–visible absorption measurements were obtained on a Cary 1 or Cary 5 spectrometer at room temperature, and baseline corrections were performed. The laser flash photolysis system, employed to measure the triplet–triplet absorption and decay kinetics of the transients, has been described previously [16]. Samples were excited by an excimer laser (Lumonics EX-510) at 308 nm or a YAG laser (Spectra Physics GCR-12) at 355 nm. The laser energy was attenuated to minimize the contribution of triplet–triplet annihilation to the triplet decay. All experiments were performed at $20\pm2$ °C. Samples in 7 mm × 7 mm Suprasil cells were purged with nitrogen for at least 15 min.

### 2.3. Fluorescence

Steady state fluorescence spectra were collected with a Perkin–Elmer MPF-66 or PTI QM-2 spectrofluorometer at $20.0\pm0.5$ °C. The emission and excitation slits were set such that the bandwidths were between 4 and 10 nm. A PTI LS-1 nanosecond single-photon counter (SPC) was employed to measure the fluorescence lifetimes at $20.0\pm0.5$ °C. The instrument response function was obtained with a suspension containing finely ground silica at the excitation wavelength employed for the fluorenone derivatives. The count accumulation was kept below 2% of the excitation rate, and 10 000 counts were accumulated at the channel of highest intensity. Decays were analyzed using the PTI software and the goodness of fit was judged by the values of $\chi^2$, $Z$ and the Durbin–Watson parameter, as well as by visual inspection of the weighted residuals and the autocorrelation function [17,18]. All samples were excited at 285 nm and the emission and excitation slits were set such that the bandwidths were between 20 and 30 nm.

The fluorescence quantum yield ($\phi_f$) of fluorenone in acetonitrile was determined using quinine sulfate in 1 N $H_2SO_4$ as standard [19]. In turn, the quantum yield of fluorenone in acetonitrile was employed as a secondary standard to measure the quantum yields of the fluorenone derivatives. In acetonitrile, **F-2CA**, **F-4CA**, **3OHF** and **2OHF** were excited at 375 nm, **2,7DBF** and **2,7DCF** were excited at 325 nm, **4OHF** and **4MF** were excited at 418 nm and **1,3DCF** and **2,7DFF** were excited at 347 nm and 400 nm respectively. All of the fluorenone derivatives in toluene were excited at 360 nm. The absorbance of the solution containing the standard ($A_s$) or the sample ($A_u$) was adjusted to approximately 0.050, with a difference of no more than 0.001. Oxygen was removed by bubbling nitrogen for at least 15 min through the solution containing the samples and another cell containing the solvent. The absorbance was checked again and solvent was added with a gas-tight syringe if solvent evaporation had occurred. Fluorescence spectra were obtained for the original solution and after dilutions by a factor of two and four. The fluorescence quantum yields were calculated using Eq. (1)

$$\phi_f = \phi_s \frac{A_s I_u n_u^2}{A_u I_s n_s^2} \quad (1)$$

which includes the correction for the solvent refractive index ($n^2$), the integrated areas of the emission spectra ($I$) and the known fluorescence quantum yield of the standard ($\phi_s$) [19]. The values for the three different concentrations were averaged for each experiment.

Solvent Raman emission was observed for some fluorenones with low fluorescence quantum yields. For these compounds, the area was determined between wavelengths that did not contribute to the Raman emission. The ratio of this area to the total area was determined from the fluorescence spectra obtained at high fluorenone concentrations where the Raman emission was negligible. It is worth noting that care should be taken with Raman emission when measuring the fluorescence of fluorenones, since recent reports have incorrectly assigned this emission to a "fluorenone monomer" emission [20].

### 2.4. Laser-induced optoacoustic spectroscopy (LIOAS)

The LIOAS equipment was based on previously described systems [21,22]. Samples in a 10 mm × 10 mm quartz cell were placed on top of a piezoelectric transducer (Panametrics, model V-104-RB transducer, 2.25 MHz). Vacuum grease was employed to improve the transmission of the heat wave generated in the cell to the transducer. The transducer/cell pair was placed in a home-built sample holder and was not moved during the experiment. The laser beam (YAG at 355 nm) was passed through a 0.8 mm pinhole, and the laser energy was attenuated by placing aqueous potassium dichromate solutions between the pinhole and the sample cell. A small portion of the laser beam was split off into a photodiode to measure the relative energy of the laser. The signal of the transducer was amplified (Panametrics model 5670) and then recorded and averaged on a Tektronix TDS 520 oscilloscope. The signal from the photodiode was averaged in a second channel of the oscilloscope. Software, written in Labview 4 (National Instruments), was employed to synchronize the different components of the equipment, and to analyze the data.

Photoacoustic techniques have their basis in calorimetry and follow energy balance equations. If the lifetime of an excited triplet state is longer than the response time of the transducer, the energy stored in the triplet state is not released. This leads to a reduction in the signal's amplitude. The value of $\phi_{isc}E_T$ can be obtained from the following energy balance equation

$$N_A h\nu_e = \phi_f N_A h\nu_f + \alpha N_A h\nu_e + \phi_{isc}E_T \quad (2)$$

where $N_A$, $h$, $\nu_e$ and $\nu_f$ are Avogadro's number, Planck's constant, the frequency of the excitation wavelength and the average frequency of fluorescence respectively. Since fluorescence is only a minor decay pathway, the frequency corresponding to the wavelength of maximum intensity in the fluorescence spectrum was employed. The parameter $\alpha$ corresponds to the ratio between the signal intensity for the unknown sample and the signal intensity for the standard. The standard employed was *ortho*-hydroxybenzophenone [22], since it releases all absorbed energy as heat.

The unknown and standard solutions were prepared with absorbances between 0.100 and 0.150 and all experiments were performed at 20 ± 2 °C. Alternating solutions (approximately 3 ml) of the standard and unknown were placed in the cell and purged with nitrogen for 20 min. The cell was not moved during the experiments, since any change in the alignment of the cell with respect to the laser beam led to changes in the waveform of the photoacoustic signal. For each experiment, three standard and two unknown samples were measured. The signal amplitude was measured between the maximum and minimum of the largest transducer signal. A linear relationship between the signal amplitude and the laser energy was observed. The slopes were corrected by dividing by the fraction of light absorbed (Eq. (3))

$$f_{abs} = 1 - 10^{-A} \quad (3)$$

which was calculated from the absorbance values measured after data collection had been completed.

The corrected slope values for the unknown and standard were averaged and used for the calculation of $\alpha$.

## 3. Results

The fluorescence spectra of the fluorenones are broad (Fig. 1) and centered between 460 and 560 nm, with the position of the maximum depending on the solvent polarity and the substitution pattern of the fluorenone (Table 1). For **F-4CA**, **F-2CA** and **1,3DCF**, a shift in the fluorescence maximum to shorter wavelengths is observed in both acetonitrile and toluene, indicating that the energy of the first excited singlet state is increased. Most other derivatives exhibit fluorescence maxima at longer wavelengths than the parent compound, indicating that the excited singlet state energy is lower for these fluorenones. The energy of the excited singlet state of fluorenone in acetonitrile is believed to be lower than that in toluene due to stabilization of the $\pi,\pi^*$ state. This trend is observed for all substituted fluorenones, except **2OHF**.

The fluorescence quantum yield of fluorenone in acetonitrile (0.027 ± 0.002) is the same as that measured previously (0.029–0.034) [6,8,9]. All other quantum yields were obtained using fluorenone in acetonitrile as a secondary standard (Table 1). This procedure leads to more precise results, since the areas of the emission spectra for the unknown sample and fluorenone are of comparable magnitude. The quan-

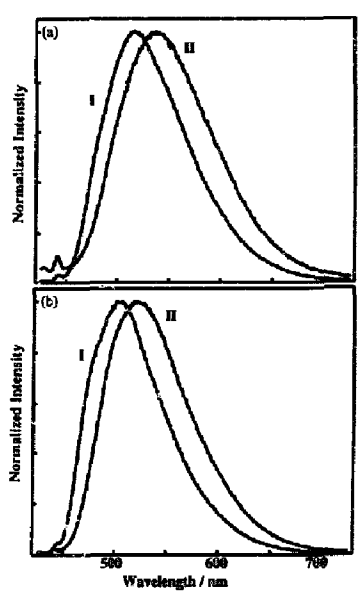


Fig. 1. Normalized fluorescence spectra of **2,7DFF** (a) and **2,7DBF** (b) in toluene (I) and acetonitrile (II).

Table 1
Fluorescence quantum yields of fluorenone derivatives in acetonitrile and toluene [a]

| Compound | Acetonitrile | | | Toluene | | |
|---|---|---|---|---|---|---|
| | $\lambda_{max}$ (nm) | $\phi_f$ ($10^{-2}$) | $\tau_f$ (ns) | $\lambda_{max}$ (nm) | $\phi_f$ ($10^{-2}$) | $\tau_f$ (ns) |
| **FL** | 510 | 2.7±0.2 | 16.5±1.5 | 490 | 0.98±0.06 | 3.6±0.5 |
| **2,7DFF** | 545 | 0.36±0.06 | 4.4±0.4 | 525 | 1.6±0.1 | 10.3±0.3 |
| **2,7DCF** | 530 | 2.4±0.2 | 8.5±1.2 | 510 | 6.0±0.5 | 13.9±0.4 |
| **1,3DCF** | 495 | <0.26±0.04 | 1.1±0.1, 9.6±0.1 [b] | 460 | 0.020±0.00[illegible] | [c] |
| **2,7DBF** | 530 | 0.9±0.1 | 2.7±0.1 | 510 | 0.96±0.05 | 1.7±0.2 |
| **2OHF** | 530 | 0.22±0.05 | [c] | 535 | 1.0±0.1 | 4.3±0.2 |
| **3OHF** | 560 | 3.2±0.4 | 13.5±0.5 | 500 | <1.2±0.1 | 2.7±0.5, 7.5±0.8 [b] |
| **4OHF** | 510 | 2.8±0.2 | 7.0±0.5 | 500 | 4.9±0.3 | 8.4±0.6 |
| **4MF** | 530 | 2.9±0.2 | 6.0±0.1 | 510 | 6.7±0.5 | 10.1±0.3 |
| **F-2CA** | 490 | 3.2±0.2 | 9.1±0.8 | 470 | 0.87±0.02 | [c] |
| **F-4CA** | 500 | 1.4±0.1 | 8.4±0.1 | 485 | <0.28±0.02 | <1 ns, 4.0±0.3 [b] |

[a] All measurements are an average of at least two determinations. For experiments performed twice, the errors were calculated as average deviations, while other errors correspond to standard deviations. Errors for $\lambda_{max}$ are ±5 nm.
[b] Biexponential decays.
[c] Compounds with low quantum yields or not sufficiently soluble to measure the lifetimes reliably.

tum yield of fluorenone emission in toluene, using fluorenone in acetonitrile as a standard, is the same as that determined previously in toluene (0.0097) [9] and benzene (0.010) [8]. In contrast with the non-substituted fluorenone, the quantum yields of several derivatives are smaller in acetonitrile than in toluene.

The fluorescence lifetimes were determined from single-photon counting experiments, and most decays were mono-exponential. The lifetimes of fluorenone in acetonitrile and toluene are similar to those observed previously [8,9]. For several fluorenone derivatives with low quantum yields and/or low solubility, we were unable to measure reliable lifetimes. In the case of **1,3DCF** in acetonitrile and **F-4CA** in toluene, a biexponential decay is observed, where the major contribution ($A_1 > 0.97$ for $A_{total} = 1$) is attributed to the short-lived species. The long-lived component is probably due to small amounts of fluorenone as an impurity. Since the long-lived emission will have a significant contribution to the steady state spectrum, the quantum yields measured should be considered as upper limits. In the case of **3OHF** in toluene, a non-exponential decay is observed which can be adequately fitted to the sum of two exponentials with similar pre-exponential factors. The emission decay for **3OHF** in acetonitrile fits very well to a first-order function. One explanation for the non-exponential decay could be the presence of dimers or aggregates of **3OHF** in toluene, which would be more prominent at the much higher concentrations necessary for lifetime measurements.

The intersystem crossing efficiency can be obtained from photoacoustic measurements, provided that the triplet lifetime is much longer than the response time of the transducer, so that the energy stored in the triplet state is not released as heat. For this reason, we measured the triplet excited state lifetimes of the fluorenones. The triplet states absorb in the 400–500 nm region with an additional weak absorption above 600 nm. Triplet decays were measured at the absorption maxima in the 400–500 nm region. A second-order contribution due to triplet–triplet annihilation was frequently observed, and was minimized by decreasing the laser pulse energy. The triplet lifetimes are in excess of 5 μs, and frequently shortened by the residual amount of oxygen in solution. Triplet–triplet absorption signals are observed for all fluorenone derivatives, except for **F-2CA** in toluene, as a result of its limited solubility in this solvent.

The values of $\phi_{isc}E_T$ were determined from the linear dependence of the amplitude of the transducer signal (inset in Fig. 2) on the laser energy (Fig. 2). The maximum laser energy employed was such that no deviation from a linear relationship between the signal's amplitude and the relative laser energy was observed. Any data for which the linear dependence deviated considerably from the origin, as well as

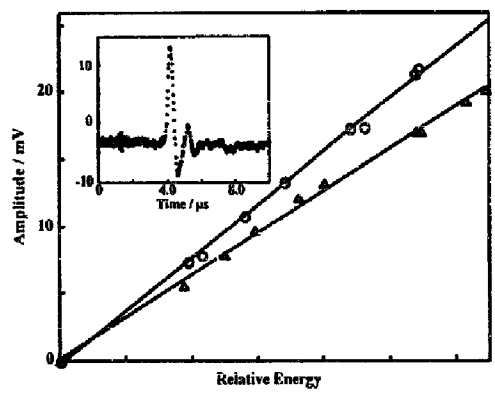


Fig. 2. Dependence of the photoacoustic signal of the standard *ortho*-hydroxybenzophenone (upper trace) and **4MF** in toluene (lower trace) on the relative energy of the laser pulse. A typical waveform is shown in the inset.

Table 2
Product of the intersystem crossing quantum yield and triplet energy, intersystem crossing quantum yield and internal conversion quantum yield of fluorenone derivatives

| Compound | Acetonitrile | | | Toluene | | |
|---|---|---|---|---|---|---|
| | $\phi_{isc}E_T$ (kcal mol$^{-1}$) | $\phi_{isc}$ | $\phi_{ic}$ | $\phi_{isc}E_T$ (kcal mol$^{-1}$) | $\phi_{isc}$ | $\phi_{ic}$ |
| **FL** | 17±3 | 0.34 | 0.63 | 36±1 | 0.68 | 0.31 |
| **2,7DFF** | 4±2 | <0.1 | >0.9 | 0±2 | <0.1 | >0.9 |
| **2,7DCF** | 7±2 | 0.14 | 0.84 | 11±1 | 0.21 | 0.73 |
| **1,3DCF** | 47±3 | 0.93 | 0.07 | 43±2 | 0.81 | 0.19 |
| **2,7DBF** | 32±4 | 0.64 | 0.35 | 28±2 | 0.53 | 0.46 |
| **2OHF** | 2±2 | <0.1 | >0.9 | −7±5 | <0.1 | >0.9 |
| **3OHF** | −1±2 | <0.1 | >0.9 | 29±6 | 0.54 | 0.45 |
| **4OHF** | 3±3 | <0.1 | >0.9 | 13±1 | 0.24 | 0.71 |
| **4MF** | −2±3 | <0.1 | >0.9 | 16±8 | 0.30 | 0.63 |
| **F-2CA** | 23±1 | 0.46 | 0.51 | [a] | [a] | [a] |
| **F-4CA** | 21±3 | 0.42 | 0.57 | 36±3 | 0.68 | 0.32 |
| **2FF** [b] | [c] | 0.16 | 0.83 | [c] | 0.72 | 0.26 |
| **2MF** [b] | [c] | 0.05 | 0.95 | [c] | 0.16 | 0.83 |

[a] Not soluble.
[b] From Ref. [14].
[c] Not measured.

data for which a change in waveform (e.g. broadening or sharpening) was observed within one set of experiments, were not considered.

The $\phi_{isc}E_T$ values are affected by the substitution pattern on the fluorenone and by the solvent polarity (Table 2). The precision of the photoacoustic method decreases as the value of $\phi_{isc}E_T$ decreases, since this product is related to the difference in slope between the standard and the sample. Any value of $\phi_{isc}E_T$ below 5 kcal mol$^{-1}$ could not be reported with confidence, and so a lower limit was set for the fluorenone values of $\phi_{isc}$ to approximately 0.1. Triplet energies of 53.3 and 50.4 kcal mol$^{-1}$ were measured from the phosphorescence spectra at low temperatures (77 K) in methylcyclohexane–isopentane (5:1) [23] and ethanol [24] respectively. The fluorenone $\phi_{isc}$ values, assuming the triplet energies ($T_1$) determined at low temperature, are calculated to be 0.34±0.06 in acetonitrile and 0.68±0.02 in toluene. Our values are lower than those determined previously (0.46±0.04 and 0.48 in acetonitrile and 0.88±0.08 in toluene) [8,9]. In these earlier experiments, triplet–triplet absorption was employed and an intersystem crossing quantum yield of unity for fluorenone in methylcyclohexane was assumed or triplet benzophenone was used as standard. Considering that different techniques were employed, which intrinsically have different limitations, and the fact that the triplet energies for fluorenone are not precisely known, the

Table 3
Fluorescence, intersystem crossing and internal conversion rate constants of fluorenone derivatives

| Compound | Acetonitrile | | | Toluene | | |
|---|---|---|---|---|---|---|
| | $k_f/10^6$ (s$^{-1}$) | $k_{isc}/10^6$ (s$^{-1}$) | $k_{ic}/10^6$ (s$^{-1}$) | $k_f/10^6$ (s$^{-1}$) | $k_{isc}/10^6$ (s$^{-1}$) | $k_{ic}/10^6$ (s$^{-1}$) |
| **FL** | 1.6 | 21 | 38 | 2.7 | $1.9\times10^2$ | 86 |
| **2,7DFF** | 0.8 | <23 | $>2.0\times10^2$ | 1.6 | <9.7 | >87 |
| **2,7DCF** | 2.8 | 16 | 99 | 4.3 | 15 | 53 |
| **1,3DCF** | <2.4 [a] | $8.5\times10^2$ [a] | >64 [a] | [b] | [b] | [b] |
| **2,7DBF** | 3.3 | $2.4\times10^2$ | $1.3\times10^2$ | 5.7 | $3.1\times10^2$ | $2.7\times10^2$ |
| **2OHF** | [b] | [b] | [b] | 2.3 | <23 | $>2.1\times10^2$ |
| **3OHF** | 2.4 | <7.4 | >67 | [c] | [c] | [c] |
| **4OHF** | 4.0 | <14 | $>1.3\times10^2$ | 5.8 | 29 | 85 |
| **4MF** | 4.8 | <17 | $>1.5\times10^2$ | 6.6 | 30 | 62 |
| **F-2CA** | 3.5 | 51 | 56 | [b] | [b] | [b] |
| **F-4CA** | 1.7 | 50 | 68 | >2.8 [a] | $>6.8\times10^2$ [a] | $>3.2\times10^2$ [a] |
| **2FF** [d] | 1.4 | 15 | 77 | 2.0 | 67 | 24 |
| **2MF** [d] | 1.7 | 30 | $6.8\times10^2$ | 2.2 | 31 | $1.9\times10^2$ |

[a] Shortest lifetime employed for calculation.
[b] Lifetime not available.
[c] Non-exponential decay.
[d] From Ref. [14].

differences between the $\phi_{isc}$ values are not sufficiently significant to invalidate any of these methods.

Photoacoustic measurements are useful in providing trends in the intersystem crossing quantum yields. However, in order to determine precise values of these yields, the triplet energy must be known. Although the reported triplet energies for fluorenone were determined from phosphorescence data [23,24], we were unable to detect, with our experimental set-up, any phosphorescence at low temperature from fluorenone and its derivatives. This inability to detect phosphorescence from fluorenone has also been reported by others [8], and is probably due to the low phosphorescence quantum yields of these compounds. The values of 50.4 and 53.3 kcal $mol^{-1}$ were used for the triplet energies in acetonitrile and toluene for all fluorenone derivatives. We are fully aware that these values are approximate. However, the intersystem crossing quantum yields (Table 2) and rate constants (Table 3) calculated using these energies are useful to identify trends in the photophysics of the fluorenone derivatives. Eq. (4) was employed to calculate the internal conversion quantum yield ($\phi_{ic}$), and the fluorescence ($k_f$), intersystem crossing ($k_{isc}$) and internal conversion ($k_{ic}$) rate constants were obtained from the relationship in Eq. (5)

$$\phi_{ic} = 1 - \phi_f - \phi_{isc} \quad (4)$$

$$k_j = \frac{\phi_j}{\tau_f} \quad (5)$$

## 4. Discussion

The solvent polarity significantly influences the photophysics of fluorenone, mainly by shifting the relative energy of $S_1$ with respect to the energy of the upper triplet state which is believed to be the $T_3$ state [7]. In non-polar solvents, $T_3$ is close in energy to $S_1$ and intersystem crossing is efficient, whereas, in polar solvents, the energy of $T_3$ is raised and the intersystem crossing quantum yield decreases.

Heavy atoms enhance spin–orbit coupling, which leads to an increase in the intersystem crossing rate constant. This effect depends on the mass of the atom, and we expect bromine to be more efficient in enhancing intersystem crossing than chlorine. A comparison of the intersystem crossing rate constants for **1,3DCF** and **2,7DCF**, which have the same number of heavy atoms, shows that the position of the substituent on the fluorenone ring is important. The $k_{isc}$ value of **1,3DCF** is much higher than that of **2,7DCF** in acetonitrile, and the same trend is observed in toluene. This suggests that the proximity of the heavy atom to the carbonyl moiety in the former compound is important in enhancing the intersystem crossing process. In fact, the $k_{isc}$ value is higher for **1,3DCF** than **2,7DBF** for which the heavy-atom effect is expected to be much more pronounced. When **2,7DCF** is compared with **2,7DBF**, the effect of the heavy atom on the intersystem crossing rate constant follows the expected behavior.

For most substituted fluorenones, an increase in the internal conversion rate constant is observed in both solvents suggesting that, regardless of the chemical nature of the substituent, the internal conversion is always enhanced. This can probably be attributed to the introduction of additional deactivation channels. In the case of the halogenated fluorenones, increases in the internal conversion and intersystem crossing rate constants influence the changes observed in the intersystem crossing quantum yields. Thus, for **2,7DCF** in both solvents, the increase in the internal conversion rate is more pronounced and the value of $\phi_{isc}$ is lower than for the parent fluorenone. In contrast, for **2,7DBF** in acetonitrile, the heavy-atom effect predominates and the intersystem crossing efficiency is high.

In addition to the arguments on how substituents influence the deactivation rate constants, we must also determine whether the relative position of $T_3$ influences the photophysical parameters measured. In analogy with previous reports, we assume that $T_3$ participates in the intersystem crossing process when an increase is observed in the $k_{isc}$ value in non-polar solvents. Since the $T_3$ excited state is $n,\pi^*$ in nature, stabilization is expected in non-polar solvents. In the case of **2,7DFF**, **2,7DCF** and **2,7DBF**, all three deactivation rate constants are similar in both solvents, suggesting that toluene does not decrease the energy of $T_3$ sufficiently for it to participate in the intersystem crossing process. As a result, there is a greater change in the $\phi_{isc}$ value in toluene than in acetonitrile, which is more pronounced than the heavy-atom effect and leads to smaller $\phi_{isc}$ values than observed for the parent fluorenone.

The additive effect of substituents can be observed when the photophysics of **2,7DFF** is compared with that of **2FF** [14]. In the case of **2,7DFF**, the intersystem crossing rate constant in toluene is smaller than that in acetonitrile, whereas for **2FF** the trend is reversed. This observation suggests that the additional fluorine leads to a widening of the energy gap between $S_1$ and $T_3$.

A comparison of the photophysical parameters for hydroxyfluorenones is not very meaningful since, in several cases, only upper limits for the intersystem crossing quantum yields are obtained. The $T_3$ state does not participate in the intersystem crossing process in toluene for the few hydroxyfluorenones which can be compared.

The effect of the nature of the substituents can be analyzed for **4OHF**, **4MF** and **F-4CA**, since the latter molecule contains an electron-withdrawing group, whereas the former have electron-donating substituents. The photophysical properties of **4OHF** and **4MF** are very similar. An $n,\pi^*$ configuration has been assigned for the $T_3$ state of fluorenone [7], and an increase in $T_3$ energy is expected with electron-donating substituents. The $k_{isc}$ values of **4OHF** and **4MF** in toluene are much smaller than that of fluorenone, indicating that the $T_3$ energy of the substituted compounds is too high to participate in the intersystem crossing process. This argument does not follow directly when analyzing the intersystem crossing quantum yields, where a higher value is observed in toluene

than in acetonitrile. However, this difference is primarily due to a relative decrease in the internal conversion rate constant in toluene, which makes it possible for the intersystem crossing process to compete. When our data for **4MF** are compared with the parameters reported previously for **2MF** [14], it is apparent that the values of $k_{isc}$ are similar, whereas an increase in $k_{ic}$ is observed for **2MF**. This increase could be due to the proximity of the electron-donating substituent to the carbonyl moiety or to a positional effect also observed with halogenated fluorenones.

**F-4CA** and **F-2CA** have electron-withdrawing substituents which stabilize excited states with an $n,\pi^*$ configuration. As a consequence, the intersystem crossing rate constants increase in toluene and acetonitrile when compared with that of fluorenone. **F-2CA** behaves in a similar fashion to **F-4CA** in acetonitrile, and no significant increase in the internal conversion rate constant is observed. This observation contrasts with the enhancement of the internal conversion process for halogen or electron-withdrawing substituents at the 2-position, suggesting that the polarizability and/or charge transfer capability of the substituent may play a role in enhancing the internal conversion process.

## 5. Conclusions

The photophysical properties of the fluorenone derivatives maintain the complexity observed for the parent compound. Certain trends in the photophysical behavior as a function of the substituent can be rationalized, but generalizations for substituents should be treated with caution since compensating effects occur. For the electron-donating substituents studied, an increase in the energy of $T_3$ with respect to the energy of $S_1$ is responsible for the removal of the solvent effect on the intersystem crossing process. However, the substituents enhance the internal conversion process to different degrees. For the electron-withdrawing substituents studied, the intersystem crossing rate constant is enhanced in toluene, probably as a result of a decrease in the energy of $T_3$. In the case of halogenated fluorenones, compensating effects are observed in which substituents increase the $T_3$ energy, leading to a decrease in $k_{isc}$, but also enhance the intersystem crossing process through the heavy-atom effect.

## Acknowledgements

This research was supported by the Natural Sciences and Engineering Research Council of Canada (NSERC). C.P.M. and R.S.M. thank the NSERC for Summer Student Research Awards. R.S.M. also thanks the University of Victoria for a Graduate Fellowship. The authors thank L. Netter for software development.

## References

[1] A. Gilbert, J. Baggott, Essentials of Molecular Photochemistry, Blackwell Scientific Publications, Oxford, 1991.
[2] A. Kuboyama, Bull. Chem. Soc. Jpn. 37 (1964) 1540.
[3] J.B. Guttenplan, S.G. Cohen, Tetrahedron Lett. (1969) 2125.
[4] R.A. Caldwell, Tetrahedron Lett. (1969) 2121.
[5] R.A. Caldwell, R.P. Gajewski, J. Am. Chem. Soc. 93 (1971) 532.
[6] L.A. Singer, Tetrahedron Lett. (1969) 923.
[7] T. Kobayashi, S. Nagakura, Chem. Phys. Lett. 43 (1976) 429.
[8] L.J. Andrews, A. Deroulede, H. Linschitz, J. Phys. Chem. 82 (1978) 2304.
[9] L. Biczók, T. Bérces, J. Phys. Chem. 92 (1988) 3842.
[10] L. Biczóc, L. Jicsinszky, H. Linschitz, J. incl. Phenom. Molec. Recog. Chem. 18 (1994) 237.
[11] T. Fujii, M. Sano, S. Mishima, H. Hiratsuka, Bull. Chem. Soc. Jpn. 69 (1996) 1833.
[12] R.S. Moog, N.A. Burozski, M.M. Desai, W.R. Good, C.D. Silvers, P.A. Thompson, J.D. Simon, J. Phys. Chem. 95 (1991) 8466.
[13] P.A. Thompson, A.E. Broudy, J.D. Simon, J. Am. Chem. Soc. 115 (1993) 1925.
[14] L. Biczók, T. Bérces, F. Márta, J. Phys. Chem. 97 (1993) 8895.
[15] N.S. Allen, S.J. Hardy, A. Jacobine, D.M. Glaser, F. Catalina, Eur. Polym. J. 25 (1989) 1219.
[16] Y. Liao, C. Bohne, J. Phys. Chem. 100 (1996) 734.
[17] D.F. Eaton, Pure Appl. Chem. 62 (1990) 1631.
[18] C. Bohne, R.W. Redmond, J.C. Scaiano, Use of photophysical techniques in the study of organized assemblies, in: V. Ramamurthy (Ed.), Photochemistry in Organized and Constrained Media, VCH Publishers, New York, 1991, p. 79.
[19] D.F. Eaton, Luminescence spectroscopy, in: J.C. Scaiano (Ed.), Handbook of Organic Photochemistry, CRC Press, Boca Raton, FL, 1989, p. 231.
[20] S. Aratha Rani, J. Sobhanadri, T.A. Prasada Rao, J. Photochem. Photobiol. A: Chem. 94 (1996) 1.
[21] S.E. Braslavsky, K. Heihoff, Photothermal methods, in: J.C. Scaiano (Ed.), Handbook of Organic Photochemistry, CRC Press, Boca Raton, FL, 1989, p. 327.
[22] S.E. Braslavsky, G.E. Heibel, Chem. Rev. 92 (1992) 1381.
[23] W.G. Herkstroeter, A.A. Lamola, G.S. Hammond, J. Am. Chem. Soc. 86 (1964) 4537.
[24] V. Huggenberger, H. Labhart, Helv. Chim. Acta 61 (1978) 250.